Dielectric Properties and Soft Modes in the Ferroelectric Mixed Crystals $K_{1-x}Na_xTaO_3$ †*

T. G. Davis
Department of Electrical Engineering and Center for Materials Science and Engineering, Massachusetts Institute of Technology, Cambridge, Massachusetts 02139
(Received 19 July 1971)

Mixed crystals of $K_{1-x}Na_xTaO_3$ undergo ferroelectric transitions for $0.05 < x < 0.72$. A maximum in the paraelectric-ferroelectric transition temperature is observed for $x \simeq 0.55$. For $0.05 < x < 0.55$, the transition is to a tetragonal ferroelectric phase. For $0.55 < x < 0.72$, the transition appears to be from cubic perovskite to an orthorhombic phase. Underdamped "soft" modes have been observed by means of Raman scattering in the paraelectric and ferroelectric phases. Raman line shapes are considerably different from those previously found in ferroelectrics, and a simple empirical expression for line shape is presented.

I. INTRODUCTION

Considerable interest in recent years has centered about observations of transverse-optical-mode instabilities associated with displacive ferroelectric phase transitions. The ferroelectric "soft" mode has been observed by means of infrared reflectivity, inelastic neutron scattering, and by Raman scattering. The displacive ferroelectrics which have been studied most extensively are $KTaO_3$,[1–5] $SrTiO_3$,[2,6–9] $BaTiO_3$,[10–13] and $PbTiO_3$.[14,15] In the case of $KTaO_3$ and $SrTiO_3$, the soft modes are well-defined underdamped modes, and the correlation between mode frequency and dielectric constant is in excellent agreement with the Cochran relation.[16] Neither $KTaO_3$ nor $SrTiO_3$, however, actually undergoes a ferroelectric transition. Raman-scattering studies in $BaTiO_3$[10] indicate that the soft mode is heavily overdamped; the scattering profile does not show a well-defined peak, but only a broad shoulder on the excitation line. In order to extract the undamped phonon frequency for correlation with the dielectric constant, a line shape must be assumed, and the resonant frequency and damping parameters determined by means of curve fitting. An underdamped soft mode has been observed in the polar phase of $PbTiO_3$ by means of Raman scattering, but no measurements were made in the cubic phase.[16] The soft mode in both phases of $PbTiO_3$ has been observed in inelastic neutron scattering, but only for values of the wave vector greater than about 8% of the Brillouin zone dimension.[14] In none of the above cases have unambiguous observations of the ($\vec{k} \simeq 0$) soft mode been made as the crystal goes through the phase transition.

We have observed by means of Raman scattering soft modes associated with ferroelectric transitions in the mixed crystal system $K_{1-x}Na_xTaO_3$. In addition to the inherent interest in soft modes in relatively disordered structures such as mixed crystals, it was possible in most cases to follow the soft mode through the phase transition.

II. DIELECTRIC AND STRUCTURAL PROPERTIES

At room temperature, potassium tantalate has the cubic perovskite structure shown in Fig. 1(a). Sodium tantalate has orthorhombic symmetry, and a multiple unit cell.[17] Ignoring the small ion displacements associated with multiplicity of the unit cell, we may represent it as shown in Fig. 1(b). The structure may be derived from a small distortion of the perovskite unit cell, consisting of a face shear of 22′ and a contraction of about 0.1% in the lattice constant in the direction perpendicular to the sheared face. The room-temperature unit-cell volumes of $KTaO_3$ and $NaTaO_3$ (as illustrated) differ by only 7.4%, and it was possible to grow mixed crystals over essentially the entire composition range.

The growth of $KTaO_3$ by a top-seeded solution technique has been described by Wemple.[18] The crystal is grown from a melt consisting of K_2CO_3 and Ta_2O_5. Optimum growth was found to occur

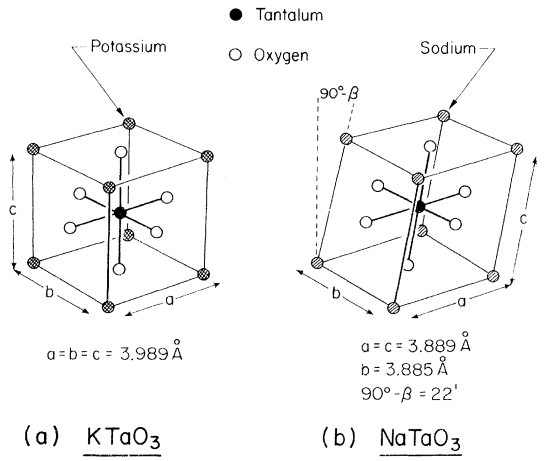

FIG. 1. Room-temperature structure of $KTaO_3$, and representation of $NaTaO_3$ structure ignoring small ion displacements associated with multiplicity of the unit cell.

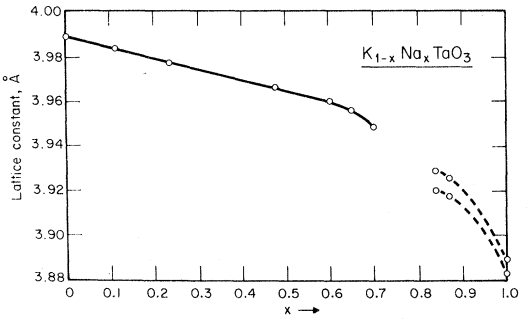

FIG. 2. Room-temperature lattice constants for the $K_{1-x}Na_xTaO_3$ system.

with about 65 mol% K_2CO_3, 35 mol% Ta_2O_5. The melt is contained in a platinum crucible in a resistance-heated furnace, with temperature controller capable of maintaining temperature to ±0.5 °C. The crystal is nucleated on a seed crystal attached to an air-cooled platinum-rhodium rod, which is slowly raised as the melt temperature is lowered at about 0.5 °C/h. We have used this method to grow mixed crystals of $K_{1-x}Na_xTaO_3$ by partial substitution of Na_2CO_3 for K_2CO_3 in the melt. The resulting crystals were typically 2–3 cm^3 in volume, with prominent {100} faces, and of high optical quality.

Mixed crystals of $K_{1-x}Na_xTaO_3$ were grown in the interval $0.02 < x < 0.92$. Crystal composition was determined by means of flame photometry. For $x < 0.72$, the room-temperature structures of the mixed crystals are cubic perovskite, with lattice constant which decreases almost linearly with x. For $x > 0.84$, the crystals are not cubic at room temperature. It is most convenient to index them as we have $NaTaO_3$: by two lattice constants and a shear angle. At $x = 0.84$, the structure appears to be tetragonal. The shear angle is at least an order of magnitude less than that observed for $NaTaO_3$. As x increases, the ratio of lattice constants decreases, and the shear angle increases to the value found in $NaTaO_3$. In Fig. 2, the room temperature lattice constants are shown as functions of composition.

For the range $0.05 < x < 0.72$, the mixed crystals undergo ferroelectric transitions, indicated by (approximate) Curie-Weiss dependence of the dielectric constant, and hysteresis below the temperature at which the peak of the dielectric constant occurs. Dielectric-constant data were taken at 1 kHz, using a G. R. 716-C capacitance bridge, and sample holder with temperature stabilized to ±0.2 °K. The estimated error is ±1%.

Figure 3(a) shows the reciprocal of the dielectric constant ($\times 10^4$) as a function of temperature for $KTaO_3$, and for mixed crystals $x = 0.12$ and 0.24. As the Curie temperature increases, deviations from the Curie-Weiss law decrease, tending to confirm the hypothesis, originally due to Barrett,[19] that deviation from Curie-Weiss behavior, often observed in ferroelectrics having transition temperatures below (50–100) °K, is specifically due to quantum effects which may be observed only at low temperatures.

Figure 3(b) shows $10^4/\kappa$ for crystals containing 48, 60, and 65 mol% $NaTaO_3$. The plateau observed in the 48 mol% sample is due to a mixture of domain orientations. If the sample is poled by application of a dc field just below the transition temperature, then the field removed, the small-signal dielectric-constant data show two distinct peaks, indicating two phase transitions. Further increase in $NaTaO_3$ concentration results in a decrease in Curie temperature, and consequent deviations from the Curie-Weiss law. The dielectric phase diagram for the mixed crystals containing between 0 and 70 mol% $NaTaO_3$ appears in Fig. 4. For compositions which contain less than 30 mol% $NaTaO_3$, there is a single ferroelectric phase transition from a cubic perovskite phase to a tetragonal ferroelectric phase, labeled ferroelectric I in the figure. The Curie temperature increases monotonically with $NaTaO_3$ concentration. Between 30 and 55% $NaTaO_3$ substitution, the crystals undergo two ferroelectric phase

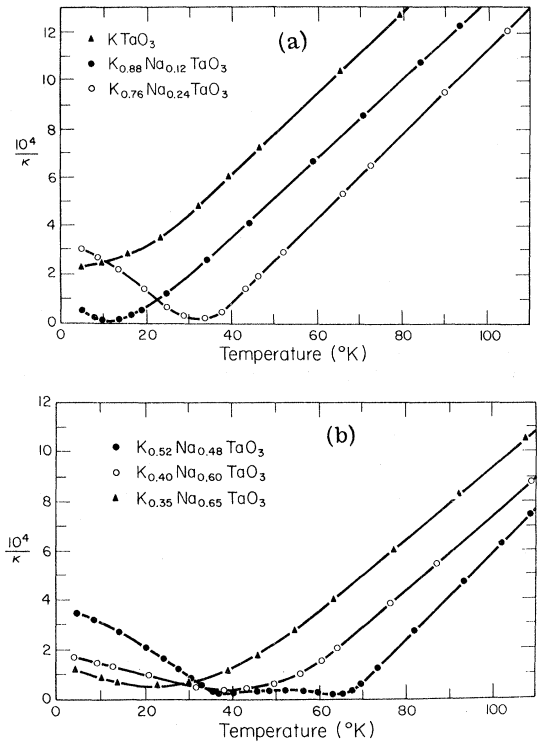

FIG. 3. Reciprocal of the dielectric constant ($\times 10^4$) for $K_{1-x}Na_xTaO_3$: (a) $x = 0$, 0.12, 0.24; (b) $x = 0.48$, 0.60, 0.65.

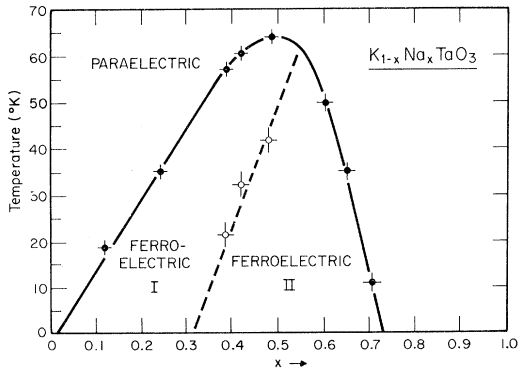

FIG. 4. Dielectric phase diagram for $K_{1-x}Na_xTaO_3$. Open circles indicate temperature of transitions from one ferroelectric phase to another.

transitions: a cubic-tetragonal transition, followed by a lower temperature transition to a ferroelectric phase of lower symmetry, labeled ferroelectric II in the figure. The lower-symmetry phase appears to be orthorhombic, but we have not yet confirmed this by x-ray diffraction. Crystals containing more than 55 mol% $NaTaO_3$ make transitions directly from the paraelectric phase into the lower-symmetry ferroelectric-II phase, and further increase in sodium tantalate concentration results in a decrease in Curie temperature. All the paraelectric-ferroelectric transitions are second order, as evidenced by absence of thermal hysteresis in the dielectric-constant data and by positive P^4 term in the Devonshire expansion of the free energy measured by field dependence of small-signal dielectric constant. The Curie constant is approximately the same for all compositions: $c = (6.0 \times 10^4)\,^\circ\mathrm{K}$.

The transition temperatures in Fig. 4 were determined by extrapolation of Curie-Weiss dependence from higher temperatures. The exact temperature of the phase transition is difficult to determine from hysteresis-loop measurements, since spontaneous polarization is small near the transition temperature, and hysteresis loops did not show distinct saturation. For $0.20 < x < 0.55$, the extrapolated Curie-Weiss temperature corresponds closely to the peak of the dielectric constant. For other compositions, particularly those having $x > 0.55$, the dielectric constant shows a broad maximum, which occurs as much as 10 °K below the extrapolated Curie temperature. Assigning the transition temperature to the maximum of the dielectric constant would result in only minor changes in the phase diagram, however, because the slope of Curie temperature vs composition is so large for $x > 0.55$.

No crystals were grown for $0.74 < x < 0.84$. Crystals having the compositions $x = 0.74$ and $x = 0.84$ showed more strain than other compositions, and more difficulty was encountered in their growth. It is possible that there is a miscibility gap in this region. Since the primary interest was in crystals which undergo ferroelectric transitions, no special effort was made to grow crystals in this interval.

For $x > 0.84$, the crystals are not cubic at room temperature. They do not undergo ferroelectric transitions, but do have weak Curie-Weiss behavior of the dielectric constant. They exhibit optical domain structure at room temperature, but no dielectric hysteresis is observed at fields up to 30 kV/cm. The optical domain structure disappears at a phase transition occurring at 220 °C for $K_{0.16}Na_{0.84}TaO_3$, and at progressively higher temperatures as the $NaTaO_3$ concentration is increased. The transition temperature for $NaTaO_3$ is 480 °C. There are no anomalies in dielectric constant at the transition, and no double hysteresis could be observed near the transition temperature with fields of 30 kV/cm. These observations do not preclude the possibility that the observed phase changes are second-order antiferroelectric transitions; we have not pursued further the investigation of the nonferroelectric compositions.

III. RAMAN SCATTERING

A. Mode Symmetry

Since a mixed crystal does not have translational invariance, $\vec{k}$ is not rigorously a good quantum number. Theoretical investigations of scattering from binary solid solutions indicate, at least in the limit of low concentration of one component, that the primary result of nonconservation of $\vec{k}$ should be a broadening of Raman lines from long-wavelength phonons owing to coupling to other modes of higher k value.[20,21] Operationally, then, we may treat the mixed crystals as if a Brillouin zone were well defined.

It is possible for a mixed crystal to exhibit more Raman lines than a single-component crystal of the same structure. In such "two-mode" behavior, Raman lines are observed in the mixed crystal with frequencies close to those of the single modes of the end members.[22,23] As is usually the case with highly ionic crystals, $K_{1-x}Na_xTaO_3$ does not show two-mode behavior. We observe in these mixed crystals a single soft mode which has the same nonzero Raman tensor elements as a single-component crystal of the same symmetry.

Neutron studies of the soft mode in $KTaO_3$ indicate that it is primarily a "Slater"-type mode.[24] That is, the mode is essentially an oscillation (at $\vec{k} = 0$) of the Bravais sublattices of oxygen octahedra and Ta ions. The soft mode in the cubic phase of mixed crystals in which sodium is substituted for potassium is presumably a perturbation of this type of mode eigenvector.

In the paraelectric phase, the cubic perovskite structure has space-group symmetry O_h^1. At zero wave vector, the representation of the soft mode is F_{1u}, which has threefold degeneracy. For nonzero wave vector (along a high-symmetry direction), the Coulomb field associated with polar phonons splits the mode into a nondegenerate longitudinal mode and a doubly degenerate transverse mode.

In the tetragonal phase, the crystal point-group symmetry is C_{4v}. The F_{1u} point-group representation of the cubic phase splits into an A_1 mode and a doubly degenerate E mode. Again, for nonzero wave vector, the Coulomb field splits the A_1 and E modes into transverse and longitudinal components. Further splitting of the E mode is possible, owing to anisotropy of the short-range forces. Phonons propagating in the z (c axis) direction may have different frequency than phonons of the same symmetry propagating in the x-y plane. In the C_{4v} polar phase, then, the soft mode may be represented as $A_1(\mathrm{TO})_{xy}+E(\mathrm{TO})_{xy}+E(\mathrm{LO})_{xy}$ for phonons propagating in the xy plane and $A_1(\mathrm{LO})_z+E(\mathrm{TO})_z$ for phonons propagating in the z direction. The terms in parentheses indicate transverse or longitudinal modes; the subscripts indicate direction of the wave vector.

The difficulty in obtaining single-domain samples precluded a study of mode symmetries in the orthorhombic phase. Birefringence of the crystal further complicates the problem of mode assignment. We have, therefore, not made a systematic study of the Raman spectrum of the lowest-symmetry phase.

B. Field-Induced Scattering

For a single-component crystal of O_h^1 symmetry, all the optical modes at $k=0$ have odd parity, and there is consequently no first-order Raman spectrum. Again, since mixed crystals do not have inversion symmetry, there is no rigorous selection rule which prohibits a first-order Raman spectrum in the paraelectric phase. We find experimentally, however, that there is no discernible first-order Raman spectrum in the cubic phase. There is an intense second-order spectrum, which for all compositions is very similar to that observed in $KTaO_3$. A study of the second-order Raman spectra of $K_{1-x}Na_xTaO_3$ has been made by Perry and Tornberg.[25]

A technique for relaxing the selection rule, making the soft mode Raman-active in the cubic perovskite phase, has been described by Fleury and Worlock.[1] The technique consists of applying an ac electric field along one of the cubic axes of the crystal, changing the symmetry from O_h^1 to C_{4v}. The additional scattered radiation synchronous with the applied field corresponds to scattering processes which are forbidden in the cubic phase.

Near the transition temperature, the small-signal dielectric constant and, therefore, the soft-mode frequency are strong functions of the applied field. In the Devonshire theory,[26] the Gibbs free energy in the cubic phase is expanded in terms of the even powers of the lattice polarization:

$$G=G_0(T)+A(T)P^2+BP^4+CP^6+\cdots \tag{1}$$

(P along one of the crystal axes). For ferroelectrics in which essentially all of the temperature dependence of the dielectric constant is attributable to temperature dependence of the soft-mode frequency, the Cochran relation becomes

$$\epsilon_0(T)=\alpha/\omega_0^2(T)\ , \tag{2}$$

where ω_0 is the soft-mode frequency and α is a constant related to the other $\vec{k}=0$ optical-mode frequencies. Using the above expression for the free energy, we have

$$\frac{1}{\epsilon_0(\kappa-1)}=\left(\frac{\partial^2 G}{\partial P^2}\right)_T=2A(T)+12BP^2+30CP^4+\cdots\ . \tag{3}$$

For second-order ferroelectric transitions, terms in P^6 and higher are usually negligible. The polarization dependence of the soft-mode frequency is then approximately

$$\omega_0(T)=[\alpha(\kappa-1)]^{1/2}[2A(T)+12BP^2+30CP^4]^{1/2}\ . \tag{4}$$

The soft-mode frequency must therefore be determined by taking the limit of $\omega_0(T)$ as the applied field approaches zero.

C. Experimental Techniques

In all the Raman-scattering experiments, the 90° scattering geometry of Fig. 5 was used. The laser beam propagates in the crystallographic [100] direction, the electric field was applied along the [001] direction, and the scattered radiation along the [010] direction was collected. This particular geometry was necessary in order to minimize effects due to inhomogeneity of crystal composition. In the growth procedure, crystals were always grown with a [010] seed orientation in the direction of pulling. Since crystal composition differs considerably from the composition of the melt, the melt composition changes during the growth process, producing a composition gradient in the direction in which the seed was pulled. Gradients in Curie temperature as large as 1–2 deg/mm were observed in some of the samples. Composition gradients in planes perpendicular to the pulling direction were at least an order of magnitude less than this value. In order to scatter from a unique value of crystal composition and electric field, it was necessary to orient the sample so that the electric field direction and direction of laser-beam propagation were both in a plane of relatively constant composition perpendicular to the growth di-

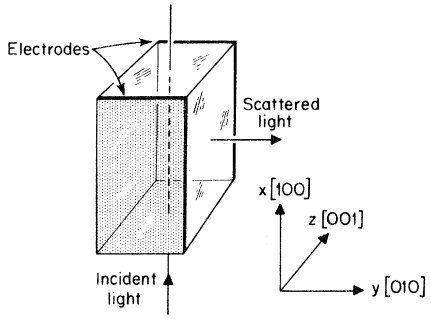

FIG. 5. Raman-scattering geometry.

rection. This means that the observed phonons propagated in the $[1\bar{1}0]$ direction. It was then geometrically possible to observe only $A_1(\mathrm{TO})_{xy}$, $E(\mathrm{TO})_{xy}$, and $E(\mathrm{LO})_{xy}$ modes.

The Raman samples were typically $2\times2\times10$ mm^3 with the laser beam entering a 2×2-mm^2 face. The electrodes were evaporated titanium, with a layer of gold evaporated over them to avoid oxidation.

A conventional exchange-gas Dewar, with sample in vacuum, was used for the experiments. Sample temperature was variable from 7 °K to room temperature, with control to ±0.2 °K.

For the electric-field-induced scattering experiments, the field applied to the sample consisted of a positive pulse, followed immediately by a negative pulse of the same amplitude and width. This was necessary in order to avoid shifting of the baseline, which might occur when pulses of one polarity are ac coupled to a nonlinear dielectric. The pulse length was variable from 0.2 to 1.0 msec, and the pulse repetition rate varied from 2 to 500 Hz. This arrangement permitted application of the same magnitude pulse at various duty factors to ensure that heating effects were negligible. The rise and fall times of the pulses were about 5 μsec, so that the period of time in which the pulse changed polarity introduced negligible error in the line shape.

Because of problems of photoconductivity, and attendent heating problems, most of the electric-field-induced scattering experiments employed a 60-mW helium-neon laser at 6328 Å as the excitation source. For scattering experiments in the polar phase a 200-mW argon-ion laser at 4880 Å was used. The scattered radiation was focused onto the entrance slit of a Spex 1400 double-grating spectrometer. A polarization rotator on the laser and analyzer on the spectrometer allowed identification of the Raman tensor element. For field-induced scattering measurements, the output of the phototube was synchronously detected in a boxcar integrator, the gate time adjusted to coincide with the entire positive-plus-negative pulse interval. For scattering in the polar phase, a conventional photon-counting scheme was used.

IV. EXPERIMENTAL RESULTS

A. Mode Frequencies in Nonpolar Phase

In $KTaO_3$ and $SrTiO_3$, it is found that essentially all the temperature dependence of the dielectric constant is due to temperature dependence of the soft mode. The Cochran relation then becomes

$$\omega_0(T) = [\alpha/\epsilon_0(T)]^{1/2}, \tag{5}$$

where ω_0 is the undamped soft-mode frequency and ϵ_0 is the low-frequency clamped dielectric constant. For $KTaO_3$ and $SrTiO_3$, the soft-mode damping is sufficiently small that the undamped phonon frequency corresponds closely to the peak of the Raman-line profile. In the case of heavy damping, the peak of the Raman line may be shifted considerably from the undamped phonon frequency. This is evidently the case in $BaTiO_3$, in which the damping is so large that the Raman line does not exhibit a peak.[10] In the $K_{1-x}Na_xTaO_3$ system, the phonon linewidths (full width at half-maximum intensity) varied from the well-underdamped case of $KTaO_3$, to cases in which the linewidths were comparable to the separation between the excitation line and the peak of the scattering response function. From the line shape, it was evident that the response function was not one which shifted the peak of the Raman line appreciably from the undamped phonon frequency. Accordingly, we have assumed the undamped soft-mode frequency to correspond to the peak of the Raman-line profile. Figures 6(a)–6(c) show the soft-mode frequencies and linewidths as functions of temperature for the compositions $K_{0.92}Na_{0.08}TaO_3$, $K_{0.70}Na_{0.30}$, TaO_3, and $K_{0.40}Na_{0.60}TaO_3$ in the paraelectric phases. For comparison, we have also shown $C/\sqrt{\kappa}$, where C is a constant chosen for the best fit. The correlation between $1/\sqrt{\kappa}$ and mode frequency is seen to be quite good even for relatively heavy damping. The linewidth increases monotonically with sodium concentration, and does not appear to be correlated with the peak in Curie temperature shown in the dielectric phase diagram. The Raman-scattering geometry was $x(zz)y$, corresponding to the Raman tensor element α_{zz}. (In the scattering geometry notation, the first letter indicates the direction of propagation of the laser beam, the letters in parentheses indicate polarizations of the incident and scattered light; the final term indicates direction of propagation of the scattered light.) The scattering is, therefore, from the $A_1(\mathrm{TO})_{xy}$ mode. The $A_1(\mathrm{LO})_z$ mode was not observable with the particular crystal orientation used. The $E(\mathrm{TO})_{xy}$ and $E(\mathrm{LO})_{xy}$ modes should have been observable in the scattering geometries $x(zx)y$ and $x(yz)y$. These modes were not found in the Raman spectrum. We conclude that the field-induced scattering from the E mode is less than 2% of the intensity observed for the

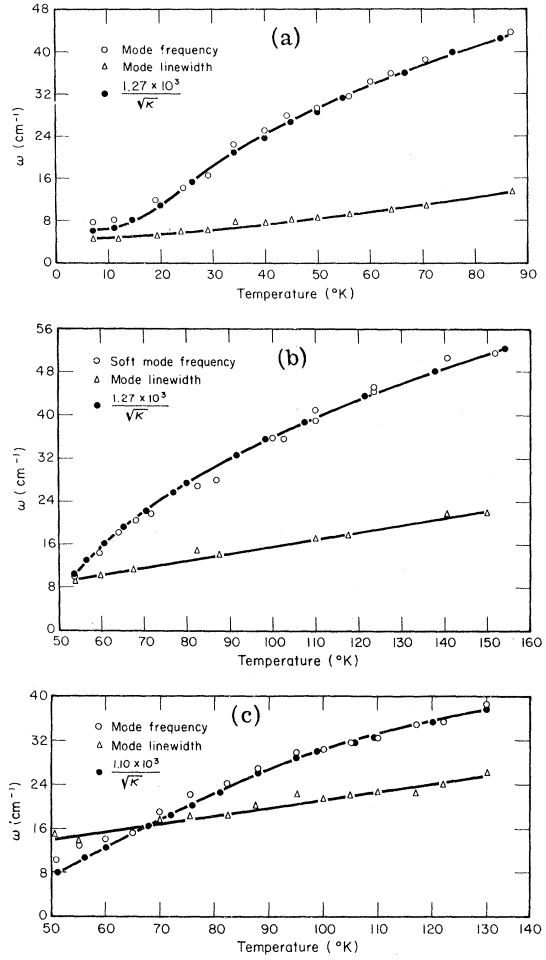

FIG. 6. Temperature dependence of soft-mode frequency and linewidth for $K_{1-x}Na_xTaO_3$. Solid circles indicate best fit to reciprocal of square root of dielectric constant: (a) $x=0.08$; (b) $x=0.30$; (c) $x=0.60$.

$A_1(TO)_{xy}$ mode.

The above data represent mode frequencies obtained in the limit of small fields. From Eq. (4), a large electric field dependence of the mode frequency is expected in the temperature interval just above the Curie point. This effect has been observed in $KTaO_3$ and $SrTiO_3$.[2] The results obtained for the mixed crystals are qualitatively quite similar to those found in $KTaO_3$. In Fig. 7, we show the mode frequency vs temperature with electric field as a parameter for $K_{0.70}Na_{0.30}TaO_3$. The general features are similar for all the mixed crystals observed. It is seen that fields of only 8 kV/cm are sufficient to increase the mode frequency by a factor of 5 at temperatures close to the transition. If we assume the Cochran relation remains valid in the case of fields large enough to cause significant shifts in the soft-mode frequency, it should be possible to calculate the constants A, B,

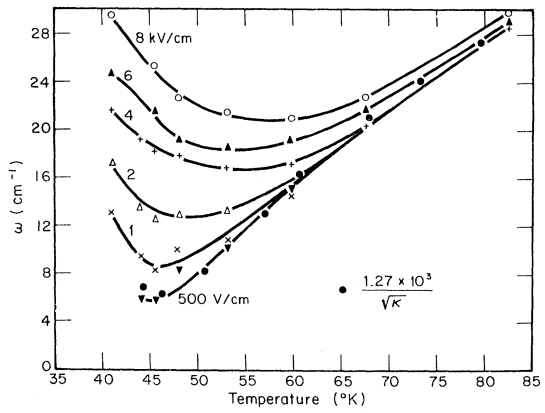

FIG. 7. Temperature dependence of soft-mode frequency in $K_{0.70}Na_{0.30}TaO_3$ with electric field as a parameter. Solid circles indicate best fit of low-field data to reciprocal of square root of dielectric constant.

and C in Eq. (4) from measurements of the field dependence of the small-signal dielectric constant. We have done such measurements using the technique of Drougard, Landauer, and Young.[27] In all cases, for fields up to 10 kV/cm, we find that C is negligible, and B is positive. This is the simplest case, and the usual one in second-order transitions.

Electric field dependence of mode frequency was not at all well described by the coefficients obtained from field dependence of the small-signal dielectric constant. In all cases, the mode frequency showed stronger field dependence than predicted, and in some cases higher-order terms were required to explain the field dependence.

B. Line Shape

In all the mixed crystals, the line shapes observed were similar. In Fig. 8, a typical Raman line is shown, with a damped harmonic oscillator

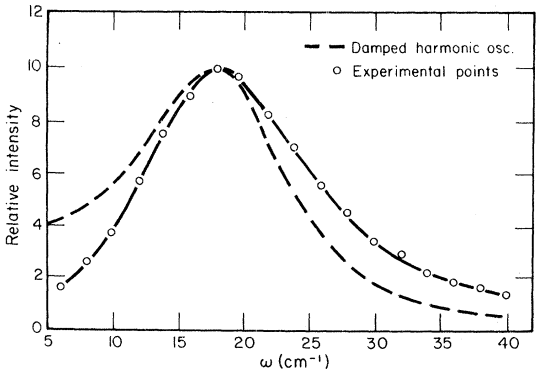

FIG. 8. Comparison of observed soft-mode profile with damped harmonic oscillator response function having same maximum and half-width.

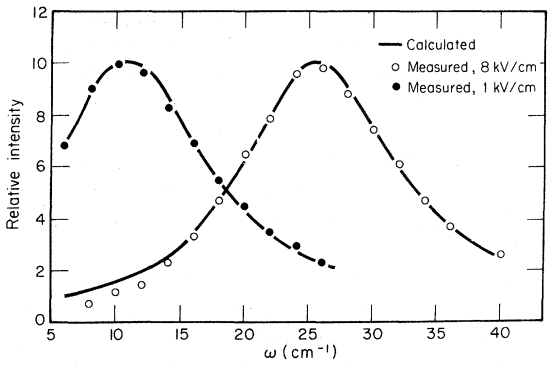

FIG. 9. Soft-mode profile in $K_{0.40}Na_{0.60}TaO_3$ at 50 °K, with applied fields of 1 kV/cm and 8 kV/cm. Damping parameter is the same in each case.

function having the same maximum and half-width for comparison. It was found that the scattering intensity was accurately described in all cases by a function of the form

$$\frac{dI(\omega)}{d\omega} = \frac{A\omega}{(\omega-\omega_0)^2+\Gamma^2}\,[\bar{n}(\omega)+1]\,, \qquad (6)$$

where $\bar{n}(\omega)$ is the Bose factor. The above line shape is for the Stokes line. The anti-Stokes line is described by the same function with $\bar{n}(\omega)+1$ replaced by $\bar{n}(\omega)$. This expression has the property that the peak of the response is close to ω_0, even for large values of Γ. For a value of Γ sufficient to give a full width at half-maximum equal to ω_0, the peak of the response is shifted up in frequency by less than 10%.

The line-shape expression is at present an empirical relation, but rather convincing evidence for its essential validity is the fact that it also describes the line shape when ω_0 is shifted by an electric field. The value of Γ is found to be independent of field strength, at least for values of E up to 10 kV/cm. In Fig. 9, the experimental points are shown for Raman scattering from the soft mode in $K_{0.40}Na_{0.60}TaO_3$ at 50 °K with applied fields of 1 and 8 kV/cm. The solid line shows the best fit to Eq. (6). The value of ω_0 has been shifted from 10.7 to 25.0 cm^{-1}, but the same value of Γ is used in each case. The contribution of the Bose factor to the line shape is quite important in this case; $\hbar\omega/kT$ varied from about 0.1 to 1.2 in the frequency interval shown on the graph.

C. Scattering in Polar Phase

In the ferroelectric phases, the crystal does not have a center of symmetry, and scattering from the soft mode is an allowed process. For Raman studies of the polar phase, a conventional photon-counting technique was used. Since photoconductive heating was not a problem in the absence of an applied field, an argon-ion laser at 4880 Å was used as the excitation source.

In all the ferroelectric samples, it was possible to observe the soft mode "stiffened" by the spontaneous polarization of the ferroelectric state. In addition, it was possible to observe the A_1-E mode splitting, which was not observable in the field-induced scattering experiments.

The most interesting soft-mode behavior was observed in crystals containing between 30 and 50% $NaTaO_3$. These compositions undergo two phase transitions, associated with two different phonon instabilities. The highest-temperature transition is from cubic to tetragonal. The second transition is from tetragonal to an orthorhombic phase, with the polar axis along a {110} direction referred to the cubic axes. This has been determined by the observation that it is possible to pole the samples completely by application of a field along a {110} direction.

Figure 10 shows the mode frequencies in the three phases of $K_{0.58}Na_{0.42}TaO_3$. The cubic-phase data are from field-induced scattering in the limit of low field. In the tetragonal phase, the soft mode is split into $A_1(TO)_{xy}$ and $E(LO)_{xy}+E(TO)_{xy}$ modes. Poling of the sample by application of a dc field prior to the scattering experiment resulted in a sample which appeared to be single domain in the scattering region. The $A_1(TO)_{xy}$ mode appeared in $x(zz)y$ geometry; the E modes were observed in $x(yz)y$ and $x(zx)y$ geometries. The A_1-mode scattering was very intense, and had the characteristic line shape of Eq. (6). The E modes were overdamped, and appeared as a broad shoulder on the excitation line. A careful line-shape analysis for the E modes has not been done; consequently, it is possible only to assign approximate upper limits to the mode frequencies. No TO-LO splitting of the E modes was observed. With decreasing tempera-

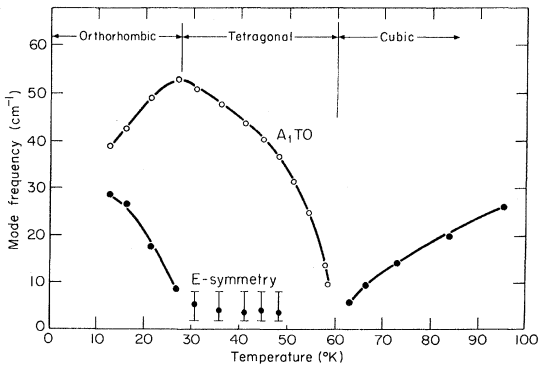

FIG. 10. Soft-mode frequencies in the three phases of $K_{0.58}Na_{0.42}TaO_3$. Data in cubic phase are from electric-field-induced scattering in low-field limit. Mode symmetries in orthorhombic phase are unknown.

ture, the A_1 mode increases in frequency, and the E modes remain overdamped.

The mode frequencies shown for the orthorhombic phase are for mixed modes of unknown symmetry and propagation direction (with respect to crystal axes), since it was not possible to pole the crystal in this phase with a field in the (001) direction. The phase transition, however, is clearly indicated by an abrupt change in polarizations in which the modes could be observed.

V. CONCLUSIONS

We have delineated the dielectric phase diagram of the mixed crystal system, and observed TO phonon instabilities associated with the ferroelectric transitions. With respect to Raman selection rules, the mixed crystal behavior is identical to that observed in single-component crystals. In all cases, the soft modes in the cubic phase show temperature dependence of mode frequencies in excellent agreement with the Cochran relation.

The dielectric phase diagram indicates the existence of a triple point occurring at the approximate composition $K_{0.45}Na_{0.55}TaO_3$. At this composition, the symmetry of the soft mode changes, and for higher sodium concentration, the soft mode condenses into an orthorhombic phase with polarization along the cubic (110) direction. Soft modes observed in field-induced scattering from mixed crystals of high sodium concentration were of A_1 symmetry; this suggests that the difference in free energies of the orthorhombic and tetragonal phases is small.

The soft-mode line shape observed in the mixed crystals is strikingly different from the damped harmonic oscillator line shapes observed in other ferroelectrics. Such line shapes may result from coupled damped harmonic oscillators; we are presently investigating this possibility.

ACKNOWLEDGMENTS

The author is indebted to Dr. N. Knable of NASA Electronic Research Center for extensive use of facilities, to Dr. A. Linz of MIT for many discussions, and to Professor A. Smakula for support during the period of research. A special acknowledgement is due V. Belruss, who grew the crystals required for the investigation.

---

†Work supported by the Advanced Research Projects Agency under contract No. DAHC15-67-C-0222 and by NASA under grant No. NGL22-001-418.

*Based in part upon thesis submitted in partial fulfillment of requirements for Ph.D., Electrical Engineering Dept., MIT, 1968.

[1]P. A. Fleury and J. M. Worlock, Phys. Rev. Letters 18, 665 (1967).

[2]P. A. Fleury and J. M. Worlock, Phys. Rev. 174, 613 (1968).

[3]J. D. Axe, J. Harada, and G. Shirane, Phys. Rev. B 1, 1227 (1970).

[4]C. H. Perry and T. F. McNelly, Phys. Rev. 154, 456 (1967).

[5]R. C. Miller and W. G. Spitzer, Phys. Rev. 129, 94 (1963).

[6]A. S. Barker and M. Tinkham, Phys. Rev. 125, 1527 (1962).

[7]R. A. Cowley, Phys. Rev. 134, A981 (1964).

[8]Y. Yamada and G. Shirane, J. Phys. Soc. Japan 26, 396 (1969).

[9]J. M. Worlock and P. A. Fleury, Phys. Rev. Letters 19, 1176 (1967).

[10]M. DiDomenico, S. P. S. Porto, and S. H. Wemple, Phys. Rev. Letters 19, 855 (1967).

[11]M. DiDomenico, S. H. Wemple, S. P. S. Porto, and R. P. Bauman, Phys. Rev. 174, 522 (1968).

[12]A. Pinczuk, E. Burstein, and S. Ushioda, Solid State Commun. 7, 139 (1969).

[13]G. Shirane, J. D. Axe, J. Harada, and A. Linz, Phys. Rev. B 2, 3651.

[14]G. Shirane, J. D. Axe, J. Harada, and J. P. Remeika, Phys. Rev. B 2, 155 (1970).

[15]G. Burns and B. A. Scott, Phys. Rev. Letters 25, 167 (1970).

[16]W. Cochran, Advan. Phys. 9, 387 (1960).

[17]I. G. Ismailzade, Kristallografiya 4, 417 (1959) [Sov. Phys. Cryst. 7, 584 (1963)].

[18]S. H. Wemple, Ph.D. thesis (MIT, 1963) (unpublished).

[19]J. H. Barrett, Phys. Rev. 86, 118 (1952).

[20]A. A. Maradudin, in *Solid State Physics*, Vol. 18, edited by H. Ehrenreich, F. Seitz, and D. Turnbull (Academic, New York, 1966).

[21]M. A. Krivoglaz, Zh. Eksperim. i Teor. Fiz. 40, 567 (1961) [Sov. Phys. JETP 13, 397 (1961)].

[22]H. W. Verleur and A. S. Barker, Phys. Rev. 149, 715 (1966).

[23]D. W. Feldman, M. Ashkin, and J. H. Parker, Phys. Rev. Letters 17, 1209 (1966).

[24]G. Shirane, J. Phys. Soc. Japan Suppl. 28, 20 (1970).

[25]C. H. Perry and N. E. Tornberg, Phys. Rev. 183, 595 (1969).

[26]A. F. Devonshire, Advan. Phys. 10, 86 (1954).

[27]M. E. Drougard, R. Landauer, and D. R. Young, Phys. Rev. 98, 1010 (1955).